NASA Technical Memorandum 101600

FREE-MOLECULE-FLOW FORCE AND MOMENT COEFFICIENTS OF THE AEROASSIST FLIGHT EXPERIMENT VEHICLE

Robert C. Blanchard

Edwin W. Hinson

July 1989

National Aeronautics and Space Administration

Langley Research Center
Hampton, Virginia 23665-5225

FREE-MOLECULE-FLOW FORCE AND MOMENT COEFFICIENTS OF THE AEROASSIST FLIGHT EXPERIMENT VEHICLE

Robert C. Blanchard
NASA Langley Research Center
Hampton, VA 23665-5225

Edwin W. Hinson
ST Systems Corporation
Hampton, VA 23665

Abstract

Calculated results for the aerodynamic coefficients over the range of $\pm 90°$ in both pitch and yaw attitude angles for the Aeroassist Flight Experiment (AFE) vehicle in free molecule flow are presented. The AFE body is described by a large number of small flat plate surface elements whose orientations are established in a wind axes coordinate system through the pitch and yaw attitude angles. Lift force, drag force, and three components of aerodynamic moment about a specified point are computed for each element. The elemental forces and moments are integrated over the entire body and total force and moment coefficients are computed. The coefficients are calculated for the two limiting gas-surface molecular collision conditions, namely, specular and diffuse, which assume zero and full thermal accommodation of the incoming gas molecules with the surface, respectively. The individual contributions of the shear stress and pressure terms are calculated and are also presented.

Nomenclature

C_A	axial coefficient
C_D	drag coefficient
$(C_D)_i$	drag coefficient for the ith element
$(C_F)_i$	components of element force coefficient along each axis (x,y,z)
C_L	lift coefficient
$(C_L)_i$	lift coefficient for the ith element
C_m	pitching moment coefficient, $C_m = (C_M)_x$
$(C_M)_j$	components of moment coefficient along each axis (x,y,z)
C_N	normal force coefficient
C_Y	side force coefficient
D	total drag force
$\bar{F}_i$	force vector acting on ith element
$\hat{i},\hat{j},\hat{k}$	unit vectors along x,y,z axis
L	total lift force
l_{ref}	reference body length (= 13.99 ft)
$\bar{M}$	total moment vector
$\bar{M}_i$	moment vector of ith element
p_i	surface pressure on ith element
p_∞	free-stream atmosphere pressure
q	dynamic pressure
$\bar{R}_i$	vector from moment reference center to centroid of ith element
S	molecular speed ratio (= 11.25)
S_i	area of ith element
S_{ref}	reference area (= 151.74 ft^2)
$\frac{T_w}{T_\infty}$	ratio of wall temperature to free-stream temperature

$\bar{V}$	velocity vector
x_b, y_b, z_b	axes of body reference system
α	angle of attack
α_i	angle of attack of ith element
β	sideslip angle
ϵ	fraction of molecules reflected specularly
θ_i	angle between velocity vector and normal to surface element
τ_i	shear stress on ith element

Introduction

An analysis of the force and moment aerodynamic coefficients in free molecule flow has been performed in support of the Rarefied-Flow Aerodynamic Measurement Experiment (RAME) being developed for the Aeroassist Flight Experiment (AFE).[1] The AFE is a subscale aeroassisted orbital transfer vehicle (AOTV)[2] being developed by NASA in order to provide flight and technology development design data for returning from geosynchronous orbit.[3] The AFE mission includes a solid rocket burn to simulate AOTV entry energy and, after a controlled energy depletion atmosphere pass, a rendezvous and retrieval by the Orbiter. The RAME is one of 12 approved experiments to be integrated into the AFE vehicle. Data from the RAME accelerometer along with other AFE measurements, including post-flight trajectory data, will be used to measure flight aerodynamic coefficients in the rarefied-flow regime including the transition into the hypersonic continuum. Several AFE attitude maneuvers are planned to explore the behavior of the free molecule flow aerodynamic coefficients with pitch and yaw attitude angles. In addition, these aerodynamic maneuvers will be performed at different altitudes and will thereby provide (for the first time) flight information on the effect that gas-surface

molecule accommodation has on aerodynamic coefficients in a changing environment (i.e., on the outbound, post atmosphere trajectory leg, the composition of the incoming gas molecules changes from mostly diatomic nitrogen to mostly atomic oxygen).

AFE Body Model

The AFE vehicle[4] consists of a raked cone aerobrake, a carrier vehicle, a solid rocket motor, and airborne support equipment. Because the solid rocket motor is fired and jettisoned prior to the RAME aerodynamic maneuver sequences, which will be performed on the outbound leg of the atmosphere pass, commencing at an altitude of about 350,000 ft., the AFE body geometry model for this analysis includes only the aerobrake and carrier vehicle, as shown in figure 1. In addition, only the forward surface of the aerobrake and the sides of the carrier vehicle are modeled because the attitude angles studied are within the range of $\pm 90°$. Thus, none of the complex aft surface of the vehicle is in the flow. For this analysis, the geometry for the forward surface of the aerobrake is taken from Cheatwood et al.[5] The equations and computer code for the sides of the carrier vehicle are based on data from reference 4. These geometry computer codes are used to generate three-dimensional coordinates for the corner points of 3,000 surface elements of the aerobrake and each of the sides of the carrier vehicle. Provisions for partial shading of the carrier vehicle by the aerobrake area also are included. Figure 2 shows the projection of the AFE model (viewer looking along the velocity vector) over the range of pitch and yaw attitude angles considered in this study.

Aerodynamic Force Coefficient Calculations

Each of the surface elements for the AFE model is treated as a flat plate whose normal vector is oriented with respect to the velocity vector through

the angle θ as shown in figure 3. The normal vector for an element is calculated from the vectors from the corner points on the AFE model surface. The angle θ is then determined by the dot product of the normal vector and the velocity vector which is defined by the attitude angles α and β as shown in figure 1. The normalized pressure on the element is taken from Bird's formulation[6] for free molecule flow, namely,

$$\frac{P_i}{P_\infty} = \left\{\frac{(1+\epsilon)}{\pi^{1/2}} S \cos\theta + \frac{(1-\epsilon)}{2}\left[\frac{T_\omega}{T_\infty}\right]^{1/2}\right\} \exp(-S^2\cos^2\theta)$$

$$+ \left\{\left[1+\epsilon\right]\left[\frac{1}{2} + S^2\cos^2\theta\right] + \frac{(1-\epsilon)}{2}\left[\frac{T_\omega}{T_\infty}\right]^{1/2}\pi^{1/2} S\cos\theta\right\}\left\{1 + \operatorname{erf}\left[S\cos\theta\right]\right\}$$

where ϵ is the fraction of molecules reflected specularly, S is the molecular speed ratio, and T_ω and T_∞ are wall and free-stream temperatures, respectively. The normalized shear stress is given by

$$\frac{\tau_i}{P_\infty} = \frac{(1-\epsilon)\, S \sin\theta}{\pi^{1/2}}\left[\exp(-S^2\cos^2\theta)^{1/2} + \pi\, S\cos\theta\{1 + \operatorname{erf}(S\cos\theta)\}\right]$$

The lift coefficient (i.e., the force coefficient perpendicular to the velocity vector) is related to the element angle of attack, α_i, by the equation

$$(C_L)_i = \frac{\left[\frac{P_i}{P_\infty}\right]\cos\alpha_i - \left[\frac{\tau_i}{P_\infty}\right]\sin\alpha_i}{S^2}, \quad 0 \le \alpha_i \le 90^\circ$$

and the drag coefficient (i.e., the force coefficient parallel to the velocity vector) is given by

$$(C_D)_i = \frac{\left[\frac{P_i}{P_\infty}\right]\sin\alpha_i + \left[\frac{\tau_i}{P_\infty}\right]\cos\alpha_i}{S^2}, \quad 0 \le \alpha_i \le 90^\circ$$

The total force components for the AFE body in the lift and drag direction are then

$$D = qC_D S_{ref} = \sum_i qS_i (C_D)_i$$

$$L = qC_L S_{ref} = \sum_i qS_i (C_L)_i$$

which yield the total force coefficients as

$$C_D = \frac{1}{S_{ref}} \sum_i (C_D)_i S_i$$

$$C_L = \frac{1}{S_{ref}} \sum_i (C_L)_i S_i$$

The normal- and axial-force coefficients are then calculated by projecting the lift and drag components onto the body axes.

Aerodynamic Moment Coefficient Calculations

The aerodynamic moment reference used in this analysis is the origin of the AFE body axis system located at the center of the reference circle, as shown on figure 1. The moment contribution of the ith surface element is

$$\bar{M}_i = \bar{R}_i \times \bar{F}$$

Where $\bar{R}_i$ is the vector from the moment reference to the centroid of the element, and $\bar{F}$ is the force vector for the element. The total moment vector is

$$\bar{M}_T = qS_{ref} l_{ref} \left[(C_M)_x \hat{i} + (C_M)_y \hat{j} + (C_M)_z \hat{k} \right] = \sum_i \bar{R}_i \times \bar{F}_i$$

which yields

$$\left[(C_M)_x \hat{i} + (C_M)_y \hat{j} + (C_M)_z \hat{k} \right] = \frac{1}{S_{ref} l_{ref}} \sum_i \bar{R}_i \times S_i \left[(C_F)_x \hat{i} + (C_F)_y \hat{j} + (C_F)_z \hat{k} \right]$$

The total moment coefficient vector calculated from this expression is then rotated into the body axis system to yield the pitch, yaw, and roll moment coefficients.

Results and Discussion

Solutions were obtained for the force and moment coefficients over the range of ±90° in both pitch and yaw separately at 10° intervals. Two limiting gas-surface molecular collsion conditions (diffuse and specular) are considered. Coefficients were calculated for the diffuse (ϵ = 0, total thermal accommodation) and the specular limit (ϵ = 1, zero thermal accommodation) to provide the extreme values of the coefficients. The shear and pressure force contributions to the total coefficient are also presented. For the results shown, the nominal values of 0.224 and 11.25 were used for the wall-to-free-stream temperature ratio and the molecular speed ratio, respectively. The diffuse coefficient calculations are insensitive to free-stream temperature ratio for all reasonable values. For example, changes in this ratio by doubling or halving only change the aerodynamic coefficients by about 2 percent maximum. Of course, the specular reflection coefficient values are totally independent of wall temperature. In addition, aerodynamic coefficient calculations are also insensitive to speed ratios above 10.

Figure 4(a) shows the variation of C_N with angle of attack for β = 0° under diffuse surface reflection conditions. Included on the figure are the two components which comprise C_N, namely, the shear stress and the pressure force. The large variation in C_N with angle of attack is due primarily to the shear stress contribution, as can be seen on figure 4(a). Figure 4(b) shows the angle of attack variation extremes of C_N for two limiting surface relection conditions, namely, completely specular reflection (ϵ = 1) and diffuse reflection (ϵ = 0). Clearly, the largest difference in the curves exist at about angles of attack of ±45°. Of course, values between the limits are possible if a combination of diffuse and specular reflection takes place.

Figures 5(a) and 5(b) show the same type of coefficient variation information for C_A as was shown for C_N in figure 4(a) and 4(b). Namely, figure 5(a) shows

the diffuse variation of C_A with angle of attack ($\beta = 0°$) and figure 5(b) shows the limits of variation of C_A with angle of attack because of surface reflection extremes. Notice in figure 5(a) that the C_A variation is primarily dominated by the pressure term. Thus, it is not surprising that the largest variation in the extreme surface reflection condition takes place at small angles of attack, as shown on figure 5(b).

To summarize, the C_N variation with angle of attack is dominated by shear stress, while the C_A variation is dominated by pressure forces. Consequently, any changes in surface accommodation will occur in C_N at large angles of attack with corresponding changes to C_A at small angles of attack. Therefore, it is expected that the ratio of C_N to C_A, shown in figure 6, displays little variation between the molecule accommodation extremes of surface reflection, since C_N and C_A effects occur at complementary angles. As seen in this figure, only at very large angles of attack (e.g., $\alpha > \pm 60°$) will differences in surface reflection take on large values. Of course, by transforming to a different orientation relative to the incoming molecule velocity, the maximum observability in surface accommodation can change. For example, shown in figure 7 is the ratio of the forces ($\beta = 0°$) in the wind axis system, i.e., C_L/C_D. Here, in this orientation, the diffuse variation is nearly maximized at $\alpha = \pm 60°$, since the specular variation is practically a constant, and very small numerically.

Figure 8(a) shows the variation of side-force coefficient, C_Y, with sideslip angle for $\alpha = 0°$. Clearly, this coefficient is also dominated by shear stress, and thus, the largest variation in surface reflection changes will occur at large side slip angles as in analogy with C_N. Figure 8(b) shows this clearly in the differences between the diffuse and specular C_Y curves.

Figure 9(a) shows the variation of C_m as a function of angle of attack for $\beta = 0°$ and diffuse surface reflection. Shown individually are the contributions of

the shear and pressure terms. As seen in this figure, the largest difference between the shear and pressure terms is at about $\alpha = -35°$ and $\alpha = 55°$. Thus, it is expected that the difference in surface accommodation would also be the largest at these angles, as seen in figure 9(b).

Concluding Remarks

The results of calculating the aerodynamic force and moment coefficients for the AFE vehicle in free molecule flow are presented for α and β ranges of $\pm 90°$. The coefficient limiting values for diffuse and specular surface reflection are also included in the data set along with the shear stress and pressure components. Examining the individual components of each coefficient suggests that C_N is dominated by shear effects and C_A by pressure effects. These effects occur at complementary angles of attack. The difference between diffuse and specular surface reflection takes on increasing values in the ratio of C_N/C_A as α increases. Thus, the largest differences are at large α's. However, transforming to the wind axis system and forming the force ratio accentuate surface accommodation effects for moderate angles of attack (i.e., $\alpha = \pm 60°$). These results support the RAME, which includes plans to make corresponding flight measurements of these coefficients during the AFE mission.

References

[1]Blanchard, R. C., "Rarefied-Flow Aerodynamics Measurement Experiment on the Aeroassist Flight Experiment," AIAA Paper 89-0630, Jan. 1989.

[2]Walberg, G. D., "A Survey of Aeroassisted Orbit Transfer," Journal of Spacecraft and Rockets, Vol. 22, No. 1, Jan.-Feb. 1985, pp. 3-18.

[3]Jones, J. J., "The Rational for an Aeroassist Flight Experiment," AIAA Paper No. 87-1508, June 1987.

[4]"Aeroassist Flight Experiment Carrier Vehicle Reference Configuration," MSFC-Doc 1610, June 22, 1988.

[5]Cheatwood, F. M., et al., "Geometrical Description for a Proposed Aeroassist Flight Experiment Vehicle," NASA TM 87714, July 1986.

[6]Bird, G. A., Molecular Gas Dynamics, Clarendon Press, Oxford, 1976.

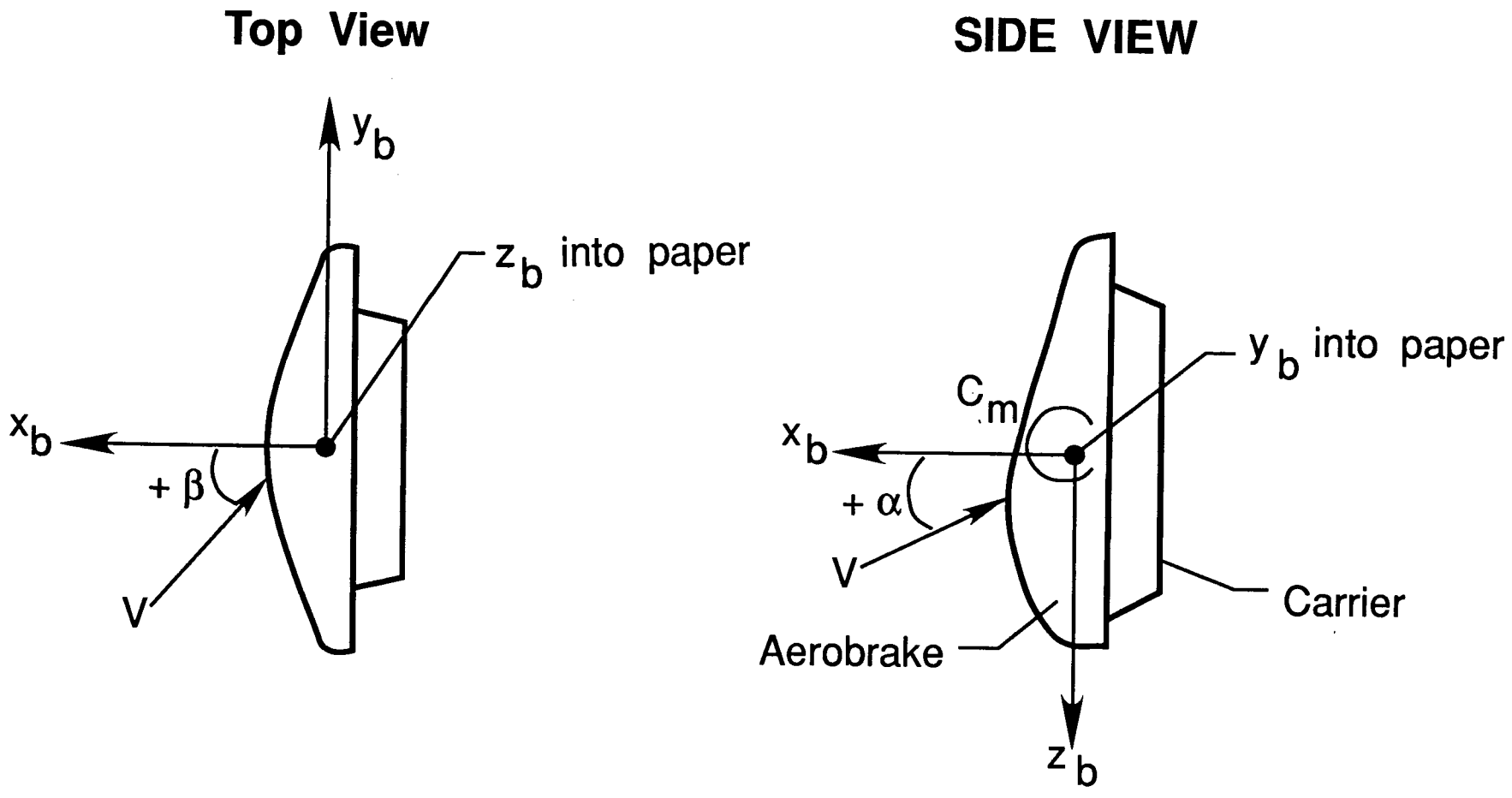

Figure 1. AFE coordinate system definition. Origin at center of reference circle.

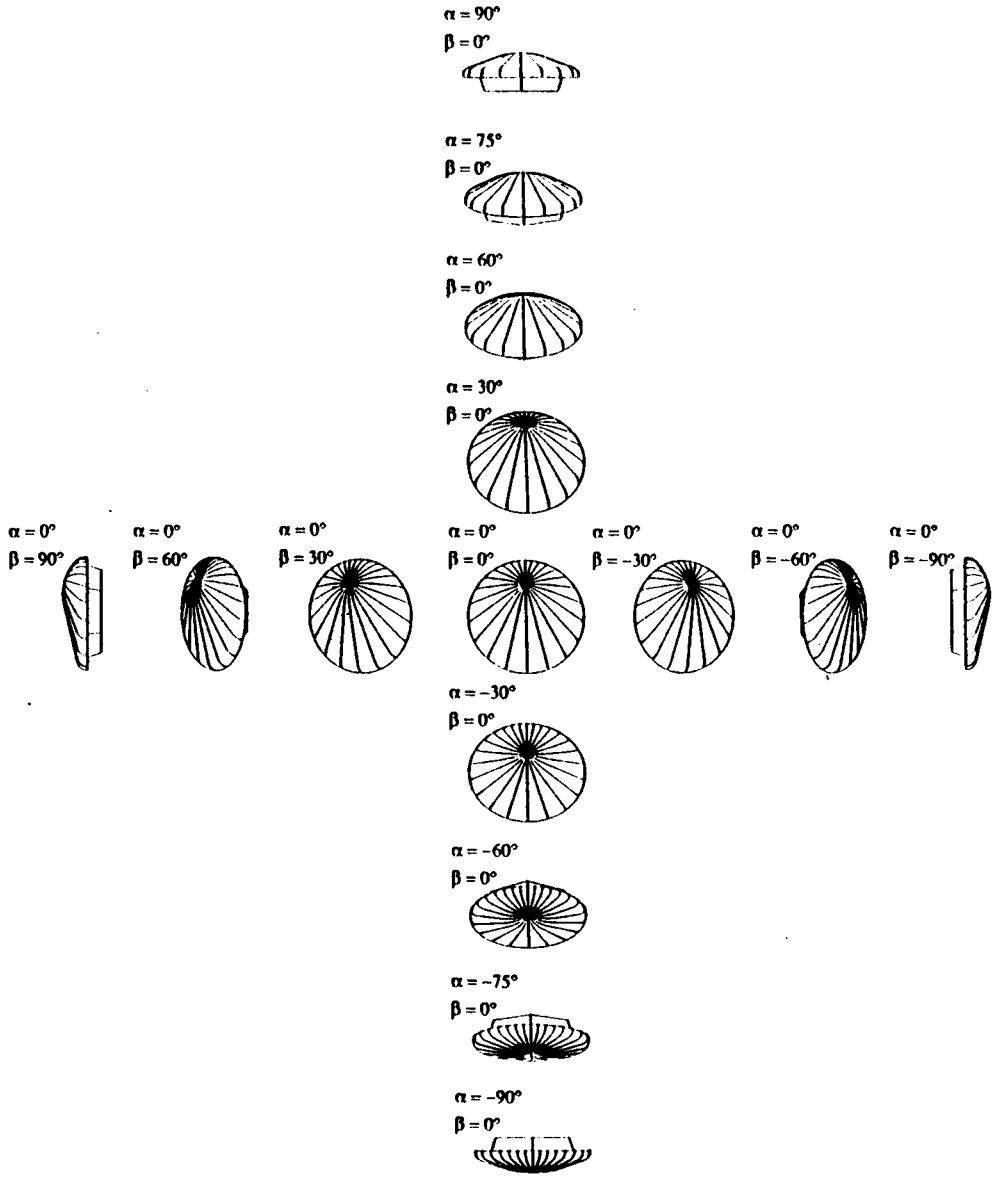

Figure 2. Orientation of AFE vehicle during RAME "α - β" maneuver sequence (velocity vector directed toward viewer).

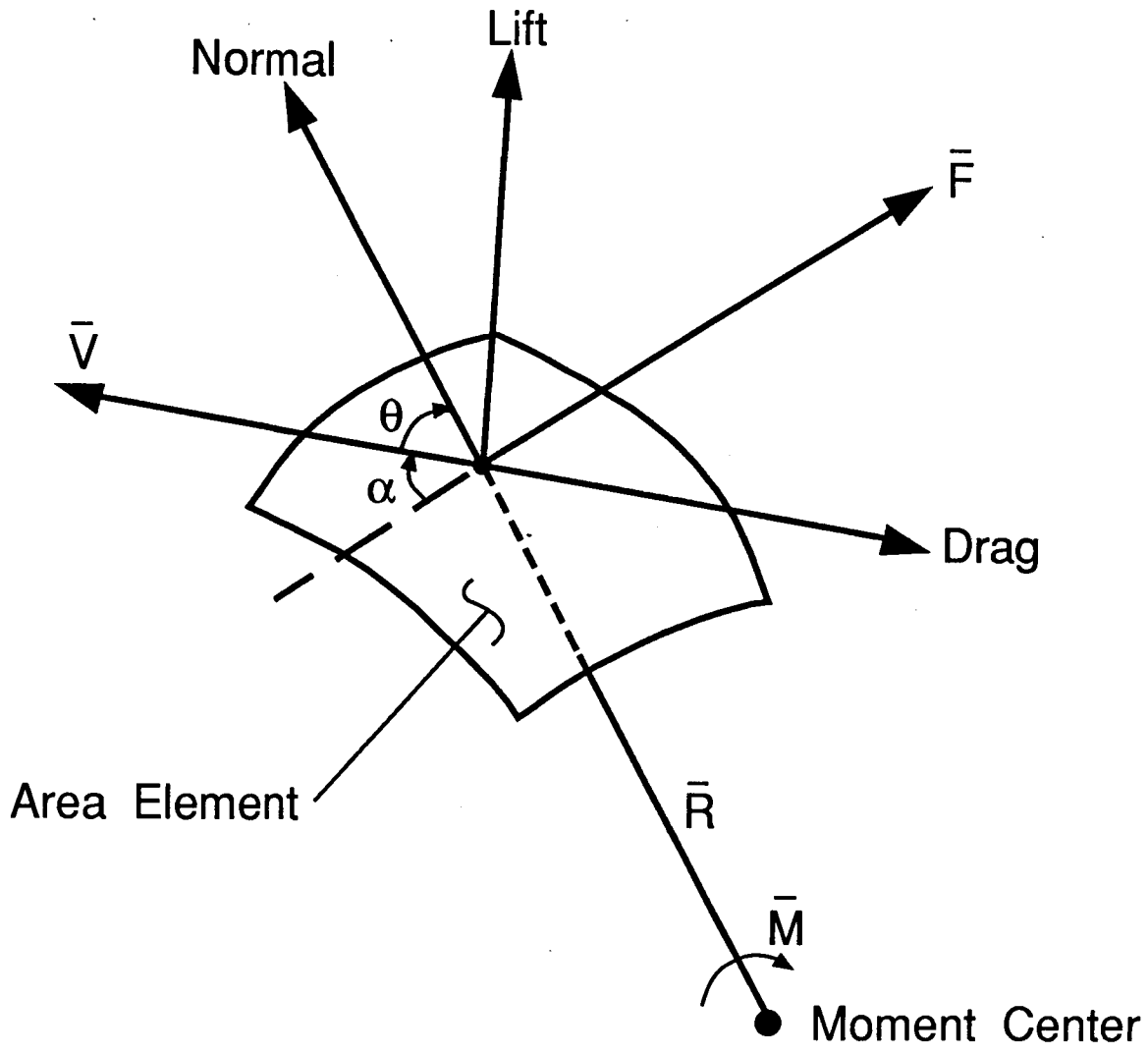

Figure 3. Element geometry.

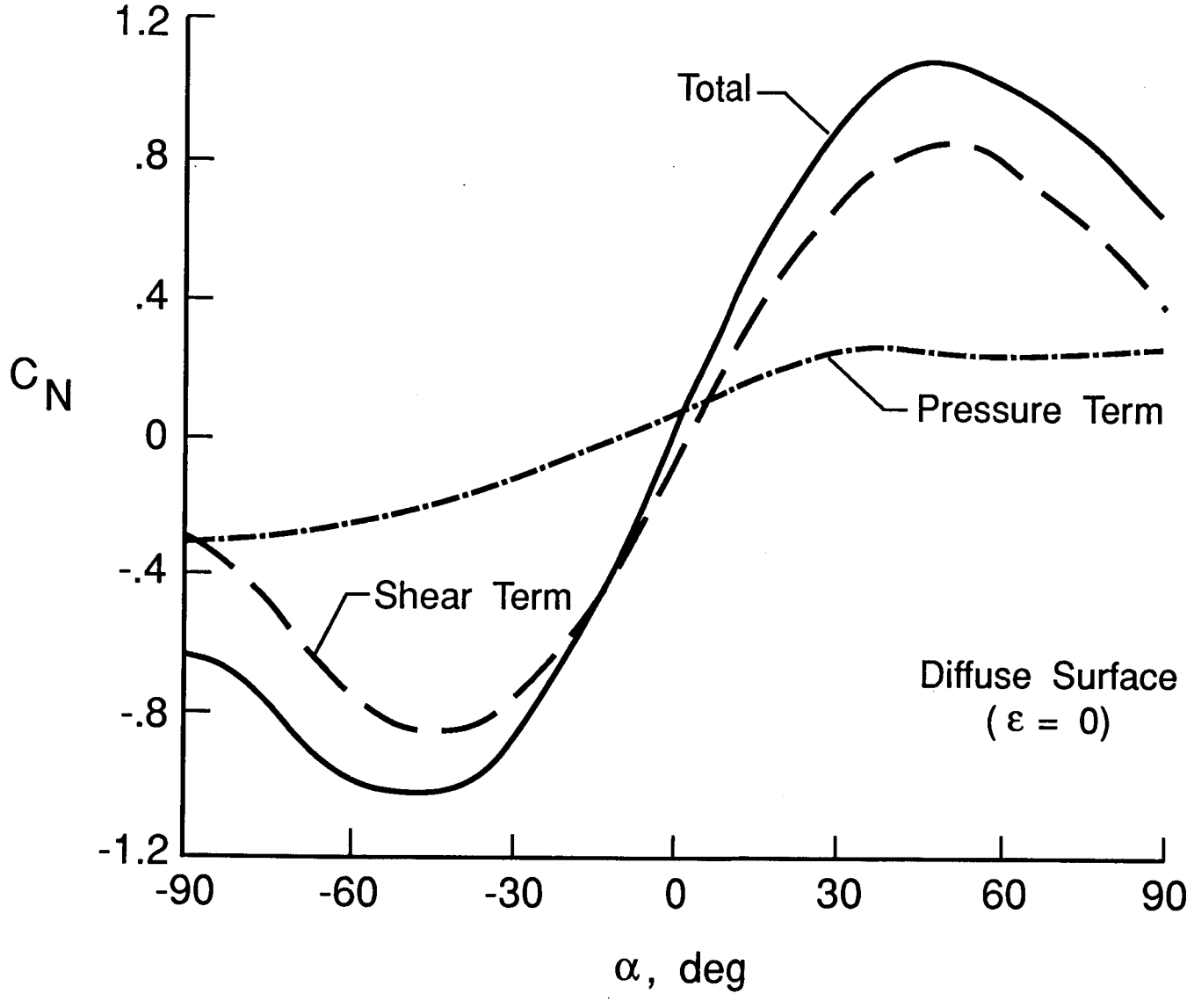

(a) C_N shear and pressure terms.

Figure 4. Variation of normal-force coefficient with angle of attack ($\beta = 0$).

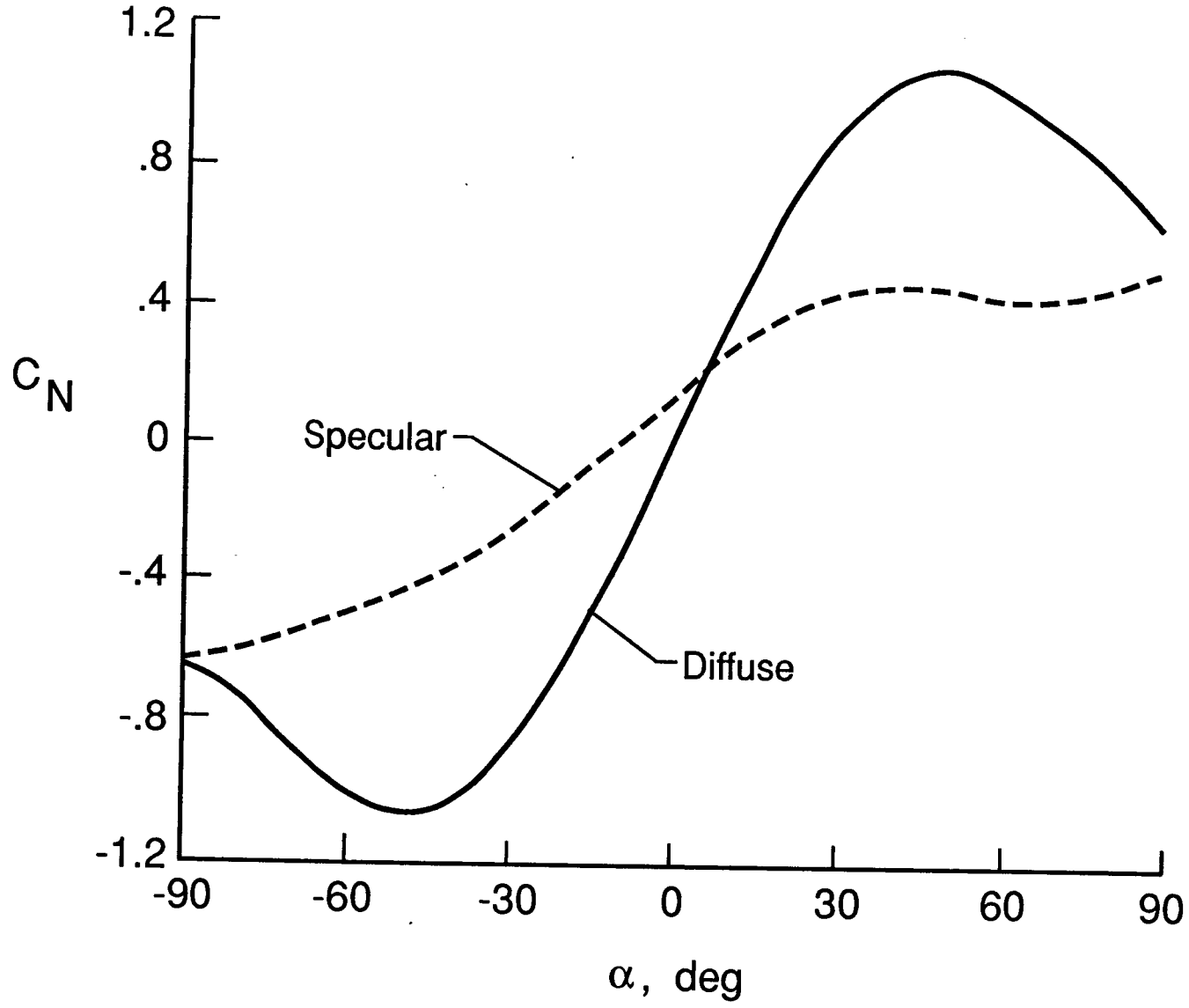

(b) Limits of C_N.

Figure 4. Concluded.

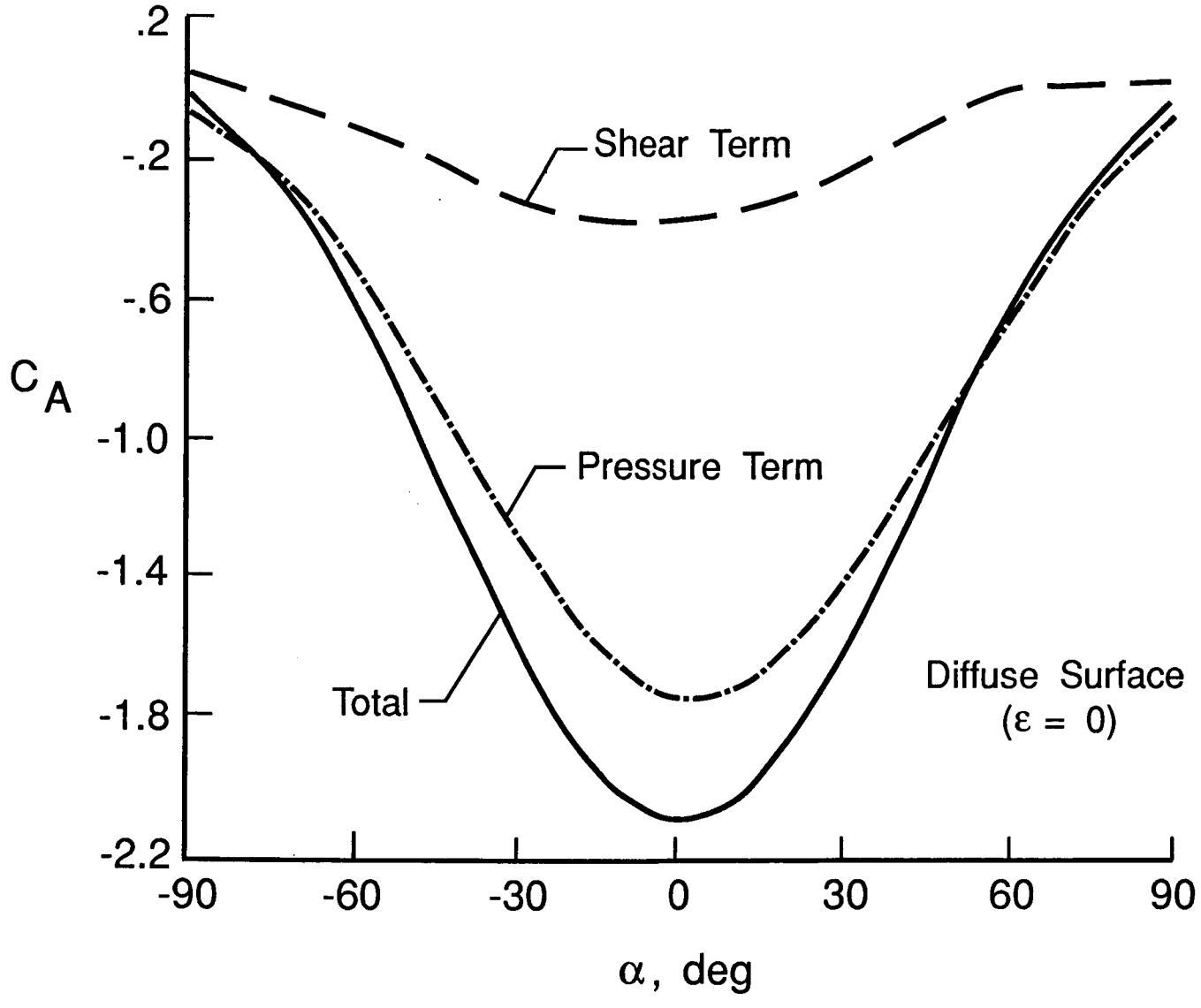

(a) C_A shear and pressure terms.

Figure 5. Variation of axial-force coefficient with angle of attack ($\beta = 0$).

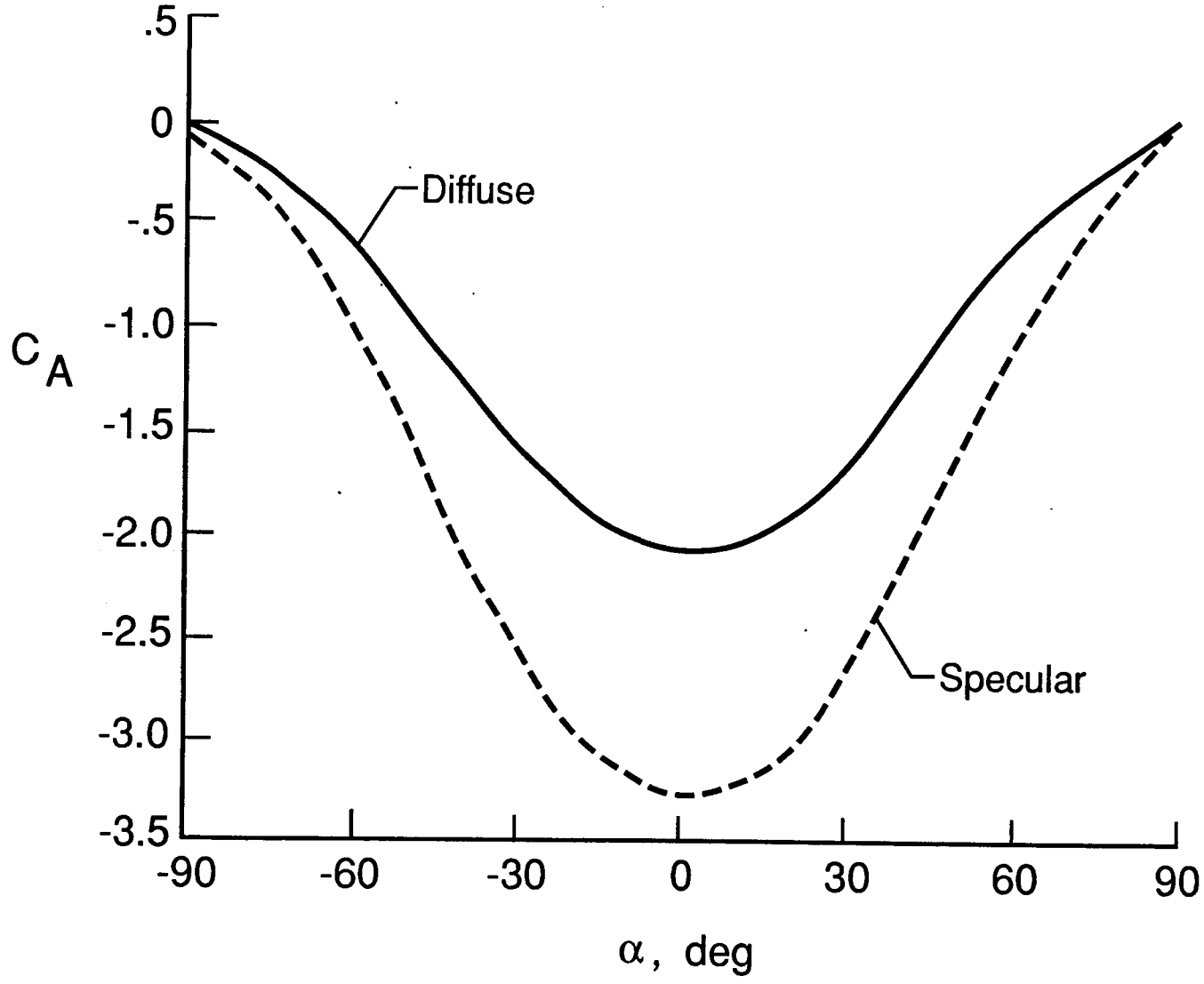

(b) Limits of C_A.

Figure 5. Concluded.

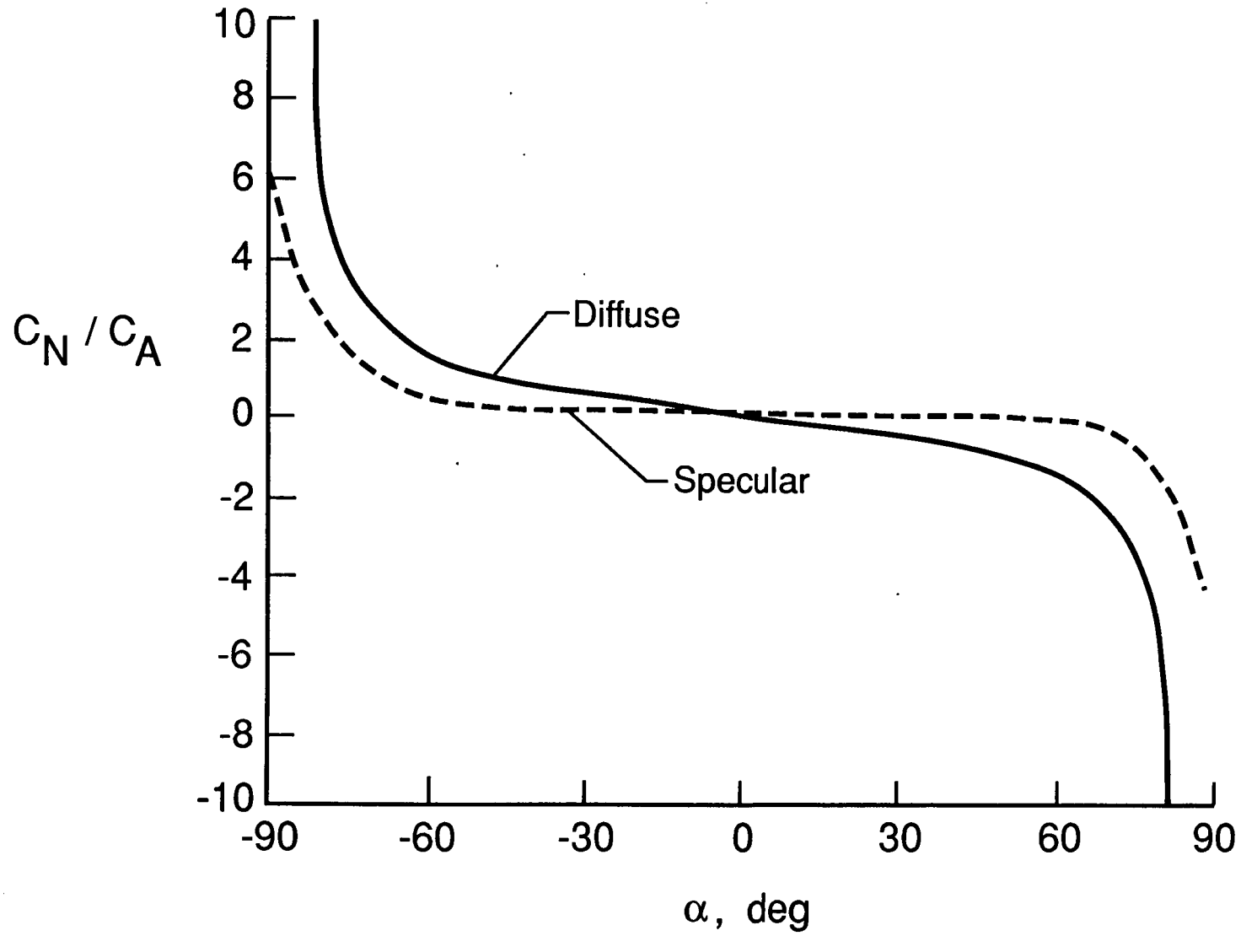

Figure 6. Variation limits of normal-force to axial-force ratio.

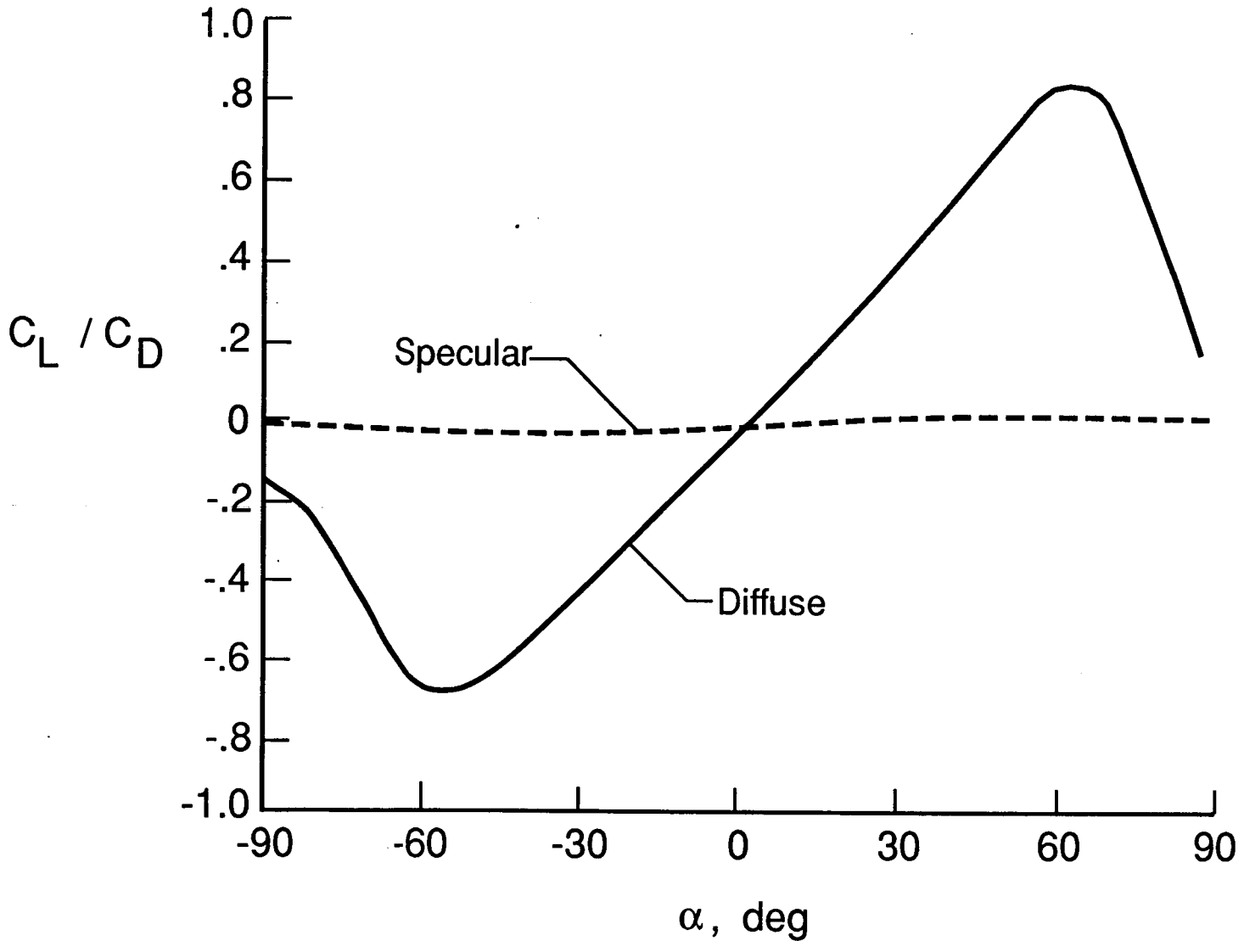

Figure 7. Variation limits of lift-to-drag ratio.

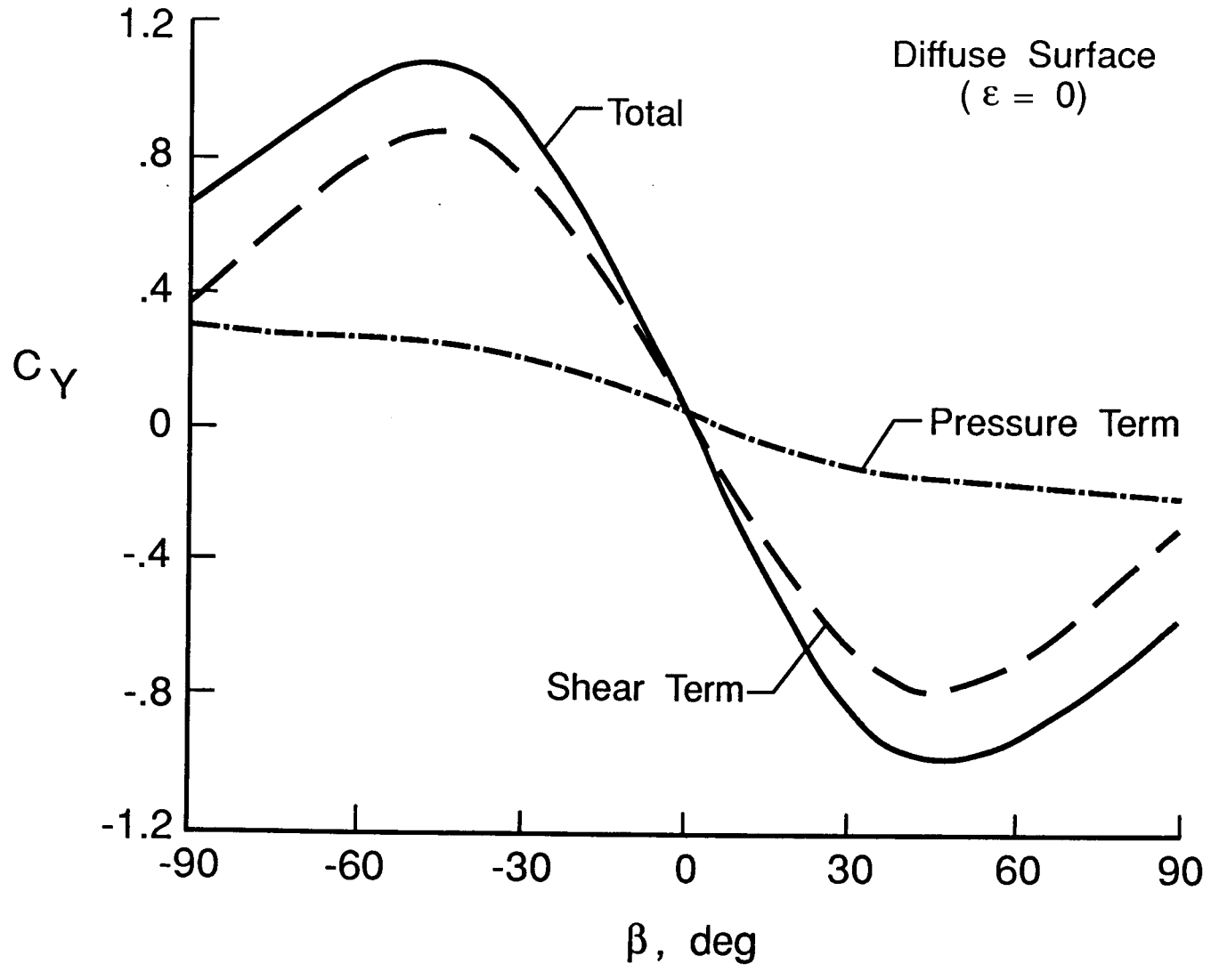

(a) C_Y shear and pressure terms.

Figure 8. Variation of side-force coefficient with angle of sideslip (α = 0).

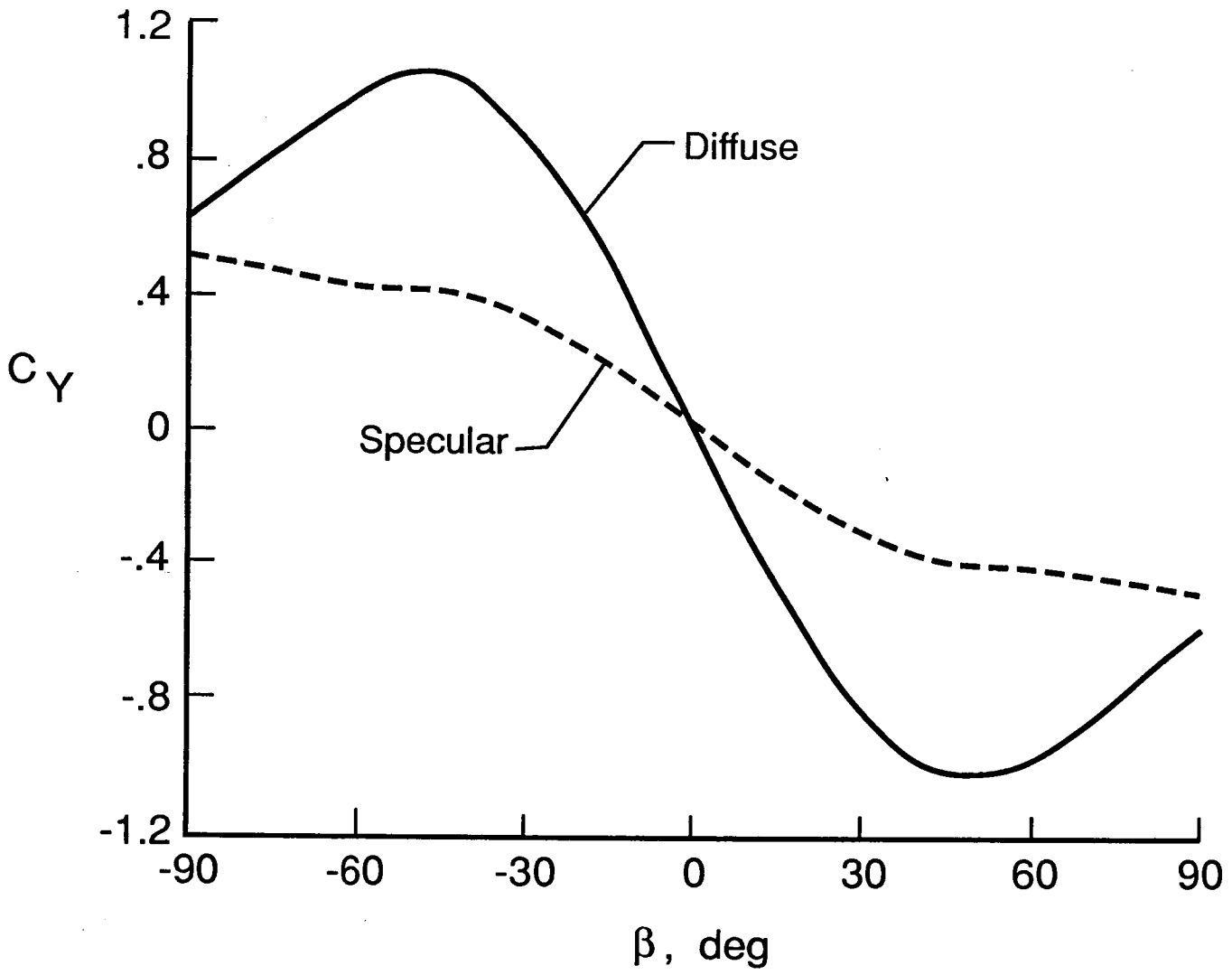

(b) Limits of C_Y.

Figure 8. Concluded.

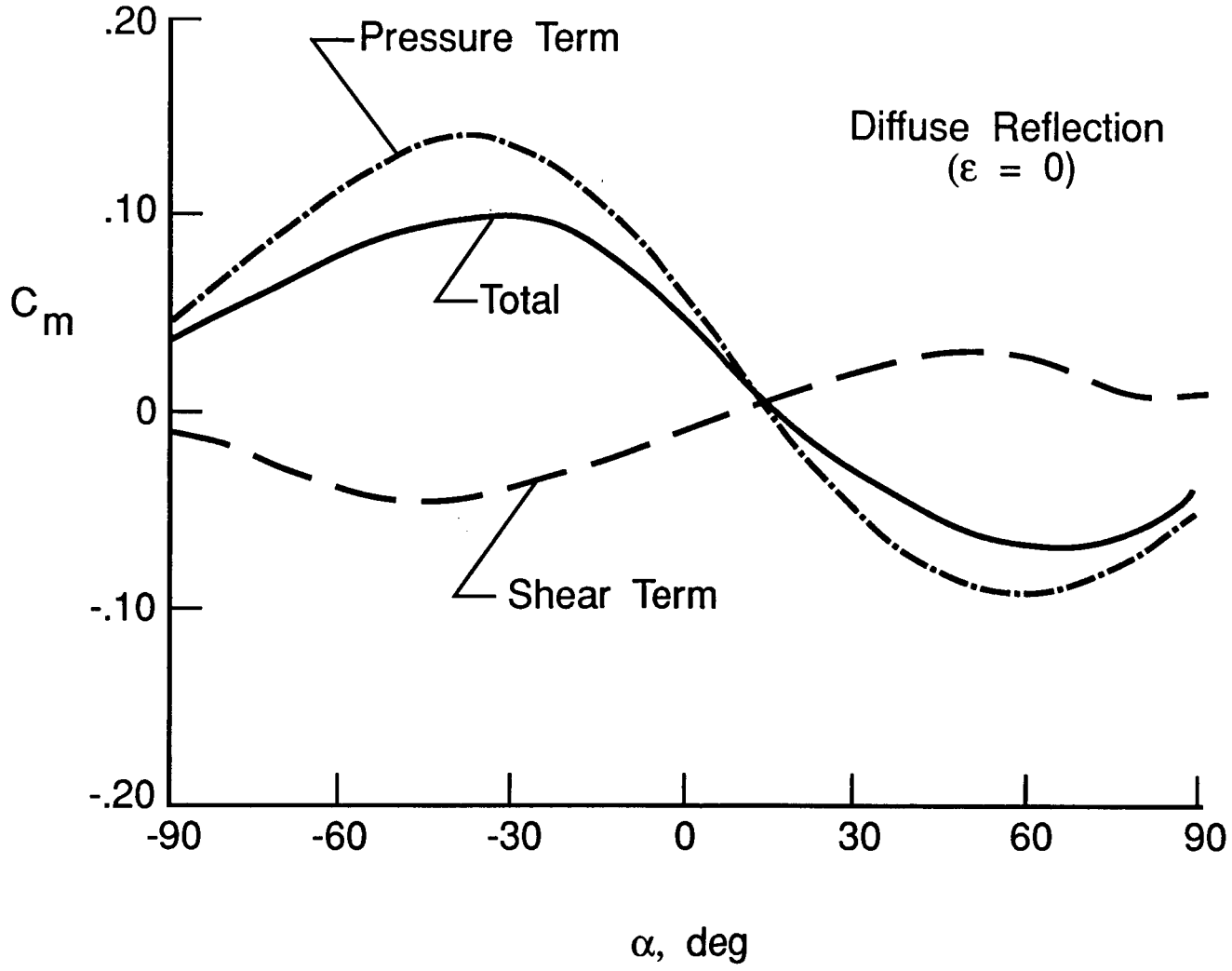

(a) C_m shear and pressure terms.

Figure 9. Variation of pitching moment coefficient with angle of attack (β = 0).

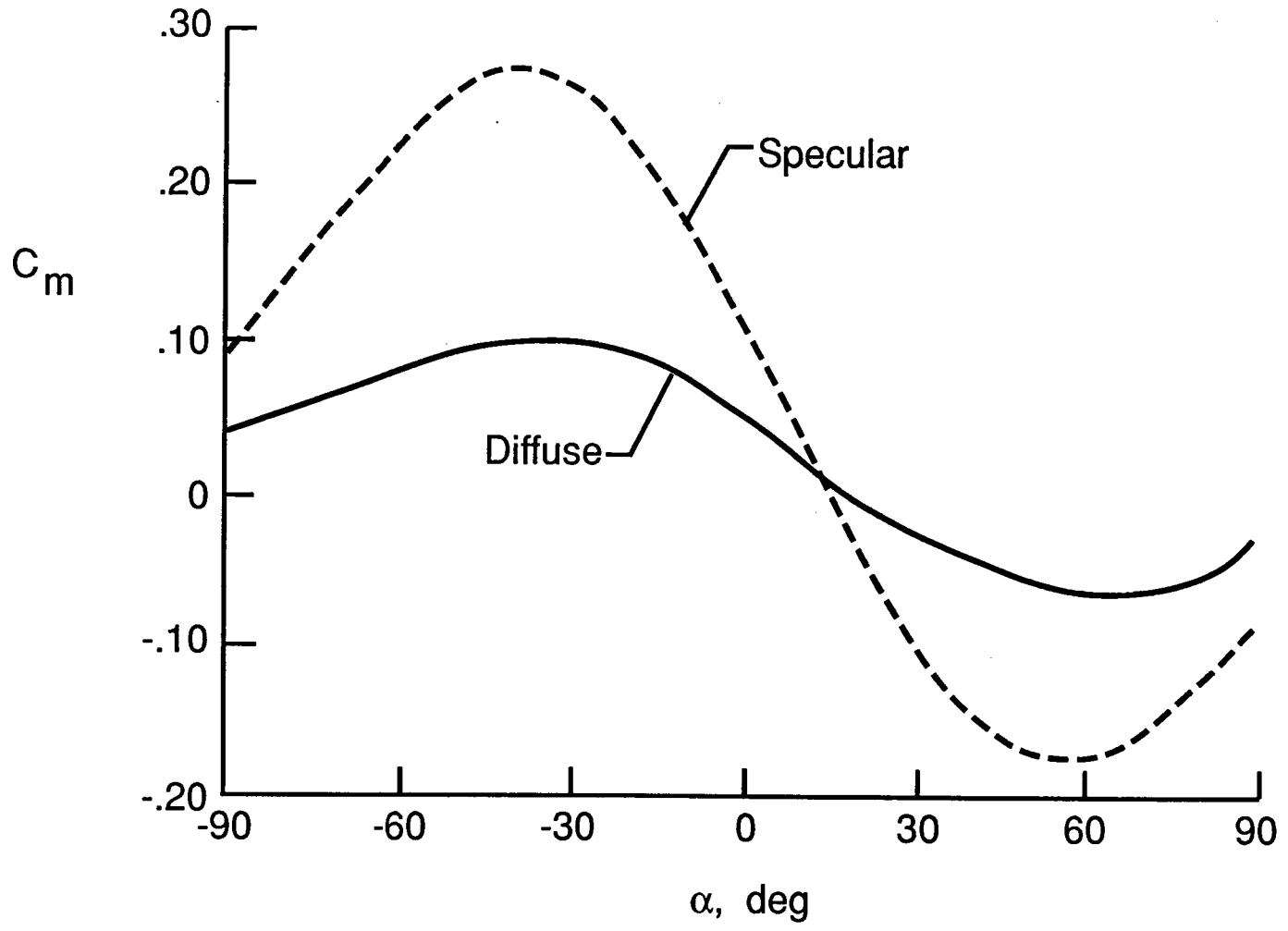

(b) Limits of C_m .

Figure 9. Concluded.

NASA National Aeronautics and Space Administration

Report Documentation Page

1. Report No.	2. Government Accession No.	3. Recipient's Catalog No.
NASA TM-101600		

4. Title and Subtitle

Free-Molecule-Flow Force and Moment Coefficients of the Aeroassist Flight Experiment Vehicle

5. Report Date

July 1989

6. Performing Organization Code

7. Author(s)

Robert C. Blanchard and Edwin W. Hinson

8. Performing Organization Report No.

10. Work Unit No.

583-01-11-05

9. Performing Organization Name and Address

National Aeronautics and
Space Administration
Langley Research Center
Hampton, VA 23665-5225

11. Contract or Grant No.

13. Type of Report and Period Covered

Technical Memorandum

12. Sponsoring Agency Name and Address

National Aeronautics and Space Administration
Washington, DC 20546-0001

14. Sponsoring Agency Code

15. Supplementary Notes

Robert C. Blanchard: Langley Research Center, Hampton, Virginia.
Edwin W. Hinson: ST Systems Corporation, Hampton, Virginia.

16. Abstract

Calculated results for the aerodynamic coefficients over the range of ±90° in both pitch and yaw attitude angles for the Aeroassist Flight Experiment (AFE) vehicle in free molecule flow are presented. The AFE body is described by a large number of small flat plate surface elements whose orientations are established in a wind axes coordinate system through the pitch and yaw attitude angles. Lift force, drag force, and three components of aerodynamic moment about a specified point are computed for each element. The elemental forces and moments are integrated over the entire body, and total force and moment coefficients are computed. The coefficients are calculated for the two limiting gas-surface molecular collision conditions, namely, specular and diffuse, which assume zero and full thermal accommodation of the incoming gas molecules with the surface, respectively. The individual contribution of the shear stress and pressure terms are calculated and also presented.

17. Key Words (Suggested by Author(s))	18. Distribution Statement
Free molecule flow Surface accommodation coefficients Aerodynamics force and moment	Unclassified-Unlimited Subject Category 02

19. Security Classif. (of this report)	20. Security Classif. (of this page)	21. No. of pages	22. Price
Unclassified	Unclassified	24	A03